Progressive Blind Deconvolution

Rana Hanocka and Nahum Kiryati

School of Electrical Engineering, Tel Aviv University
hanocka@mail.tau.ac.il

Abstract. We present a novel progressive framework for blind image restoration. Common blind restoration schemes first estimate the blur kernel, then employ non-blind deblurring. However, despite recent progress, the accuracy of PSF estimation is limited. Furthermore, the outcome of non-blind deblurring is highly sensitive to errors in the assumed PSF. Therefore, high quality blind deblurring has remained a major challenge. In this work, we combine state of the art regularizers for the image and the PSF, namely the Mumford & Shah piecewise-smooth image model and the sparse PSF prior. Previous works that used Mumford & Shah image regularization were either limited to non-blind deblurring or semi-blind deblurring assuming a parametric kernel known up to an unknown parameter. We suggest an iterative progressive restoration scheme, in which the imperfectly deblurred output of the current iteration is fed back as input to the next iteration. The kernel representing the residual blur is then estimated, and used to drive the non-blind restoration component, leading to finer deblurring. Experimental results demonstrate rapid convergence, and excellent performance on a wide variety of blurred images.

Keywords: progressive blind restoration, residual blur removal, image deblurring, piecewise-smooth image model, Mumford & Shah regularization, sparse PSF prior

1 Introduction

Image deblurring algorithms can be classified as non-blind or blind, depending on whether the blur kernel is assumed to be known or unknown. Even the milder non-blind image deblurring problem is notoriously hard, as it is essentially ill-posed. Classic approaches for non-blind deblurring, notably the Wiener filter [15], implicitly regularize the problem by imposing an image-smoothness prior. In the last decade or so, substantial progress has been achieved by incorporating more realistic image priors, requiring sophisticated algorithms and numerical techniques to solve the resulting optimization problems. Notably, the Mumford & Shah image prior (originally introduced for image segmentation [14]) favors piecewise-smooth image structure, preserving edges rather than smoothing them. Bar *et al* [4] developed a non-blind deblurring algorithm using the Mumford & Shah image prior. Their method relies on the Γ-convergence approach [3] and on advanced numerical techniques to minimize the non-trivial

free-discontinuity objective functional. As long as the blur kernel is known, the non-blind deblurring algorithm of Bar *et al* yields state of the art results, and can be computed in real time using a PC-type GPU [18].

In blind deblurring, the unknown blur kernel adds another layer of ambiguity to the already difficult non-blind problem. For decades, the blind deblurring problem was considered quite hopeless. Bar *et al* [7], followed by [5], settled for *semi-blind* deblurring, limited to estimating an unknown parameter of an otherwise specified family of blur kernels (*e.g.*, variance in the case of Gaussian blur). However, practical applications of semi-blind deblurring are limited, since physical blur kernels seldom conform with common theoretical blur models, and deblurring algorithms are sensitive to deviations from the assumed blur kernel.

Recently, there has been a new wave of blind deconvolution methods, employing powerful PSF priors [2, 6, 1, 11, 17]. While there have been significant advances in the field, the blind deconvolution problem is far from solved. Due to the sensitivity to blur-kernel estimation errors, non-blind methods usually outperform blind methods when the correct blur kernel is known. Various real-world applications still rely on manual tuning of the assumed blur kernel within a non-blind framework, e.g. [9].

We present a blind image deblurring algorithm employing the powerful Mumford & Shah image prior and a sparse PSF prior. The problem is cast in a coarse-to-fine progressive framework which inherits the elegance and sophistication of the Mumford & Shah image model, and addresses the residual image blur associated with blur-kernel estimation errors. Iterative reduction of the residual blur relaxes the accuracy requirements from the blur estimation component, reduces the need for parameter tuning, and leads the residual blur kernel to approach an impulse function. Experimental results demonstrate the applicability of the suggested approach to a wide range of deblurring challenges.

2 Variational Elements

2.1 Fundamentals

The standard blurred image formation model is

$$g = u * h + n \tag{1}$$

where g, u, h, and n denote the blurred image, latent image, blur kernel, and random additive noise, respectively. Image deblurring is the recovery of the latent image u given the blurred image g. Depending on whether the blur kernel h is known or unknown, deblurring methods are classified as either non-blind or blind. In practice, when using non-blind methods, the blur kernel must usually be estimated using side information regarding the imaging process, or by a manual trial-and-error procedure. Even in the non-blind scenario, image deblurring is an ill-posed problem, requiring regularization using a-priori assumptions regarding image structure. The deblurring problem is often formulated as a functional minimization problem, which in the non-blind case takes the form

$$F_{nb} = S(u, h, g) + Q(u) \tag{2}$$

where F_{nb} is the (non-blind) objective functional, $S(u, h, g)$ is a fidelity term that reflects the assumed noise distribution, and $Q(u)$ is the regularization term, *i.e.*, the image prior.

In blind methods, the blur kernel is unknown; thus, both the latent image *and* the blur kernel need to be recovered from the given blurred image. With an unknown blur kernel, blind image restoration is an extremely difficult, highly ill-posed problem. There have been several attempts, e.g. [19, 20], to incorporate a PSF prior in the form of an additional kernel regularization term:

$$F_b = S(u, h, g) + Q(u) + R(h) \tag{3}$$

where F_b is the (blind) objective functional and $R(h)$ is the blur-kernel prior. In principle, this functional leads to Euler-Lagrange equations that can be solved by alternate minimization. In practice, success has been rather limited. It has been argued [17] that independent PSF estimation should precede a non-blind deblurring phase. The progressive deblurring strategy suggested in this paper diverges from both previous approaches. The deblurred outcome of the current two-stage (PSF estimation + non-blind deblurring) iteration is fed back as input to the next iteration, rapidly eliminating the residual blur. We proceed to specify the fidelity and regularization terms used in the PSF estimation and deblurring components of this work.

2.2 Image Terms

The fidelity term used in this work is the standard $\mathcal{L}_2$-norm

$$S(u, h, g) = \frac{1}{2} \int_{\Omega} (h * u - g)^2 dA \tag{4}$$

that reflects the ubiquitous Gaussian noise assumption.

The image prior is adapted from the Mumford & Shah segmentation functional (5), favoring piecewise-smooth image structure. This model holds for most natural images, with the exception of extremely textured images (where the piecewise-smooth model can be applied to texture feature maps). The Mumford & Shah segmentation functional (F_{MS}) is given by

$$F_{MS}(u, K) = \frac{1}{2} \int_{\Omega} (u - g)^2 dA + \beta \int_{\Omega / K} |\nabla u|^2 dA + \alpha \int_{K} d\sigma \tag{5}$$

where Ω is the image domain, K is the edge set, and α, β are positive regularization constants. Minimizing this functional is challenging, and had been an open problem for many years, especially since the unknown edge set K appears not only in the integrand but also in the integration domain.

Ambrosio and Tororelli [3] addressed this problem via the Γ-convergence framework. The irregular functional $F_{MS}(u, K)$ is approximated by a sequence

of regular functionals $F_\epsilon(u)$ such that $F_{MS}(u,K) = \lim_{\epsilon\to 0} F_\epsilon(u)$. The edge set K is represented by a characteristic function $(1-x_K)$ which is approximated by a smooth auxiliary function $v(x)$, *i.e.*, $v(x) \approx 0$ if $x \in K$, and $v(x) \approx 1$ otherwise (not on the edges). Therefore, the functional becomes

$$F_\epsilon(u,v) = \frac{1}{2}\int_\Omega (u-g)^2 dA + \beta \int_\Omega v^2 |\nabla u|^2 dA + \alpha \int_\Omega \left(\epsilon |\nabla v|^2 + \frac{(v-1)^2}{4\epsilon}\right) dA \tag{6}$$

which can be solved using sophisticated numerical methods.

Bar *et al* [7, 4] demonstrated that image restoration and segmentation are tightly coupled tasks, and used the Mumford & Shah piecewise-smoothness terms in their Γ-convergence formulation to regularize the image deblurring problem. In the non-blind case, Bar *et al* minimized the functional

$$F(u,v) = \frac{1}{2}\int_\Omega (h*u-g)^2 dA + \beta \int_\Omega v^2 |\nabla u|^2 dA + \alpha \int_\Omega \left(\epsilon |\nabla v|^2 + \frac{(v-1)^2}{4\epsilon}\right) dA \tag{7}$$

where

$$Q_\epsilon(u,v) \equiv \beta \int v^2 |\nabla u|^2 dA + \alpha \int_\Omega \left(\epsilon |\nabla v|^2 + \frac{(v-1)^2}{4\epsilon}\right) dA \tag{8}$$

are the image regularization terms. Gildenblat [18] has shown that this elaborate functional can be efficiently minimized using GPU architecture, approaching real-time computation on low-cost hardware.

2.3 Sparse PSF Prior

The design of PSF priors for blur identification and blind restoration has attracted substantial attention in recent years [1, 6, 11, 2, 16, 17], leading to performance breakthroughs. Following Kotera *et al* [1], we model the blur with a Laplace distribution on the positive PSF values, leading to the sparse prior

$$R(h) = \int_\Omega \Psi(h(x,y))dA, \quad \Psi(h(x,y)) = \begin{cases} h(x,y), & \text{if } h(x,y) \geq 0 \\ \infty, & \text{otherwise} \end{cases} \tag{9}$$

3 Algorithm

3.1 Strategy

The proposed algorithm is an iterative process alternating between two steps. The first step consists of estimating the blur kernel h as suggested by Kotera *et al*, also disregarding the u solution. In the second step, given the current estimate of h, the latent image u and edge-map v are estimated by minimizing the non-blind functional (7).

Due to kernel estimation errors, residual blur is present after the non-blind deconvolution step. We progressively remove this residual blur, by iteratively feeding the residually-blurred image back into the system. Convergence is quick (after 1-3 iterations), and the estimated residual blur kernel approaches an impulse function, indicating that recovery of the latent image u has been finalized.

3.2 Solving for h

Estimating h within a MAP framework approaches the true blur kernel solution (given enough measurements in g and u) [17]. Therefore, we adopt a MAP approach to exploit the asymmetry between the dimensionality of the latent image u and the small (relative to u) blur kernel h. Refer to the functional minimized by Kotera *et al* [1]

$$L(u,h) = \frac{1}{2}\int_{\Omega}(h*u-g)^2 dA + Q(u) + \int_{\Omega}\Psi(h(x,y))dA \tag{10}$$

where $Q(u)$ corresponds to their gradient-based image prior. When minimizing with respect to h, the image prior $Q(u)$ vanishes, resulting in the functional

$$\min_{h}\frac{1}{2}||hu-g||^2 + R(h). \tag{11}$$

Kotera *et al* minimized this functional using the augmented Lagrangian method. A new function $\tilde{h} = h$ is introduced to separate the minimization of the data term and the PSF regularizer, leading to

$$\min_{h,\tilde{h}}\frac{\gamma}{2}||hU-g||^2 + R(\tilde{h}) \quad \text{s.t.} \quad h = \tilde{h} \tag{12}$$

where γ is a positive constant and U is a (fixed) convolutional operator constructed from u. The augmented Lagrangian method adds to the Lagrangian a quadratic penalty term for each constraint, such that the new functional we wish to minimize (after rearranging) becomes

$$\min_{h,\tilde{h}}\frac{\gamma}{2}||hU-g||^2 + R(\tilde{h}) + \frac{\zeta}{2}||h-\tilde{h}-a_h||^2 \tag{13}$$

where a_h is proportional to the estimate of the Lagrange multiplier of the above constraint in (12). This function can be minimized using coordinate descent (for additional details see Kotera *et al* [1]).

3.3 Solving for u and v

The objective functional (7) is strictly convex and lower-bounded with respect to either u or v when the other is held constant along with the PSF (h) from the previous step. Note that this convexity property holds for general blur kernels (not necessarily limited to a parametric model). The Euler-Lagrange equations for v and u are

$$F_v = 2\beta v|\nabla u|^2 + \alpha \cdot \frac{v-1}{2\epsilon} - 2\epsilon\alpha\nabla^2 v = 0 \tag{14}$$

$$F_u = (h * f - g) * h(-x, -y) - 2\beta \mathrm{Div}\left(v^2 \nabla u\right) = 0. \tag{15}$$

The objective functional is iteratively minimized by solving these equations with the Neumann boundary conditions [7].

4 Experiments

The top left image in Figure 1 is Lena, synthetically blurred with a Gaussian kernel. The blind deblurring results obtained using the algorithms of Kotera *et*

Fig. 1: Top left: blurred image. Top right: blind deconvolution using Kotera *et al* [1]. Bottom left: blind deconvolution using Shan *et al* [6]. Bottom Right: our blind restoration result.

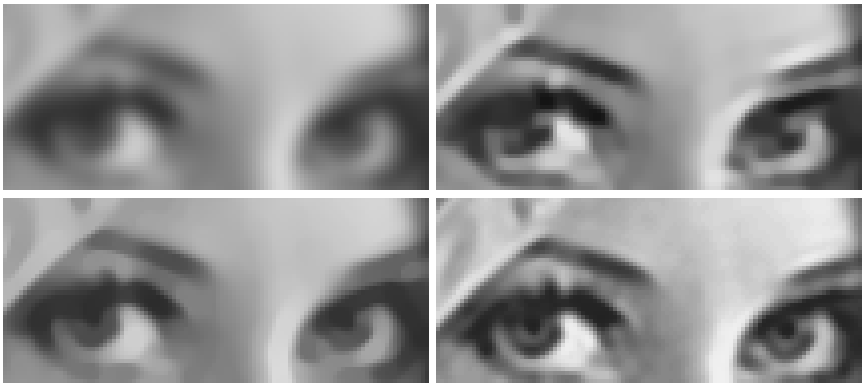

Fig. 2: Zoom in of Figure 1. Top left: blurred image. Top right: blind deconvolution using Kotera *et al* [1]. Bottom left: blind deconvolution using Shan *et al* [6]. Bottom Right: our blind restoration result. Notice the differences in the right pupil.

al [1] and Shan *et al* [6] are respectively shown in the top right and the bottom left. Our result is shown in the bottom right. While all three results are adequate, our result appears to be the best, as can be seen in Figure 2, for example near the right pupil.

The recovery of a high-quality still image from a video sequence of a static scene imaged through atmospheric turbulence is a notoriously difficult problem. Certain methods apply non-rigid registration to each frame and average the results. The outcome is a blurred average image that is commonly modeled as a latent image blurred by a space-invariant Gaussian kernel. The average image is restored using a deblurring algorithm, see *e.g.*, [9]. The top row in Figure 3 shows three such average images. The middle row is the result of non-blind deconvolution using manually optimized Gaussian blur kernels [9]. The bottom row presents our blind deconvolution result. It can be seen that the blind results are on par with the manual, painstakingly optimized non-blind reconstructions.

Figures 4 and 5 show blind deblurring of pictures taken using a smartphone with incorrect focus settings and motion blur.

The left column in Figure 6 shows three heavily blurred images, with the true blur kernel shown below each image. The right column is the outcome of the suggested progressive blind restoration algorithm. Below each of the recovered images, we show the estiamted blur in the first iteration and the residual blur estimated in the second iteration.

Running time for a 255×255 image on a $3.40\,Ghz$ Intel quadcore machine using unoptimized MATLAB is approximately 20 seconds. The algorithm converges in one to three iterations, depending on the accuracy of the initial blur kernel estimation.

Fig. 3: First row: average of a video sequence following non-rigid registration [9]. Second row: manually-optimized non-blind deconvolution result [9] (non-blind). Third row: deconvolution using the proposed blind deconvolution method. Left column: video sequence courtesy of Mahpod and Yitzhaky [12]. Right column: video sequence courtesy of Oreifej [13].

5 Conclusions

Iterative algorithms for concurrent blur estimation and image restoration, *e.g.,* [19, 20] are mathematically elegant but lead to questionable results. Following the observations of [17], sequential blind restoration is often preferred, meaning that the blur kernel is estimated first, then non-blind deblurring is applied. This approach is followed, for example, in the state of the art algorithm of Kotera *at* [1]. However, PSF estimation errors are inevitable, and image restoration is sensitive to these errors, limiting performance. We suggest an iterative blind deblurring approach, where PSF estimation and image deblurring are decoupled within each iteration, but the deblurred outcome of each iteration is fed back as the input image to the next iteration. This leads to progressive elimination of the residual blur.

The proposed blind image restoration method incorporates the Mumford & Shah piecewise-smooth image model with a sparse PSF prior. We have thus reached a goal that Bar *et al* [7] and others [5] have not been able to accom-

Fig. 4: Top row: blurred image. Second row: proposed blind deconvolution method. Third row: enlarged blurred patches. Fourth row: recovered sharp patches.

Fig. 5: Top row: blurred image. Second row: proposed blind deconvolution method. Third row: enlarged blurred patches. Fourth row: recovered sharp patches.

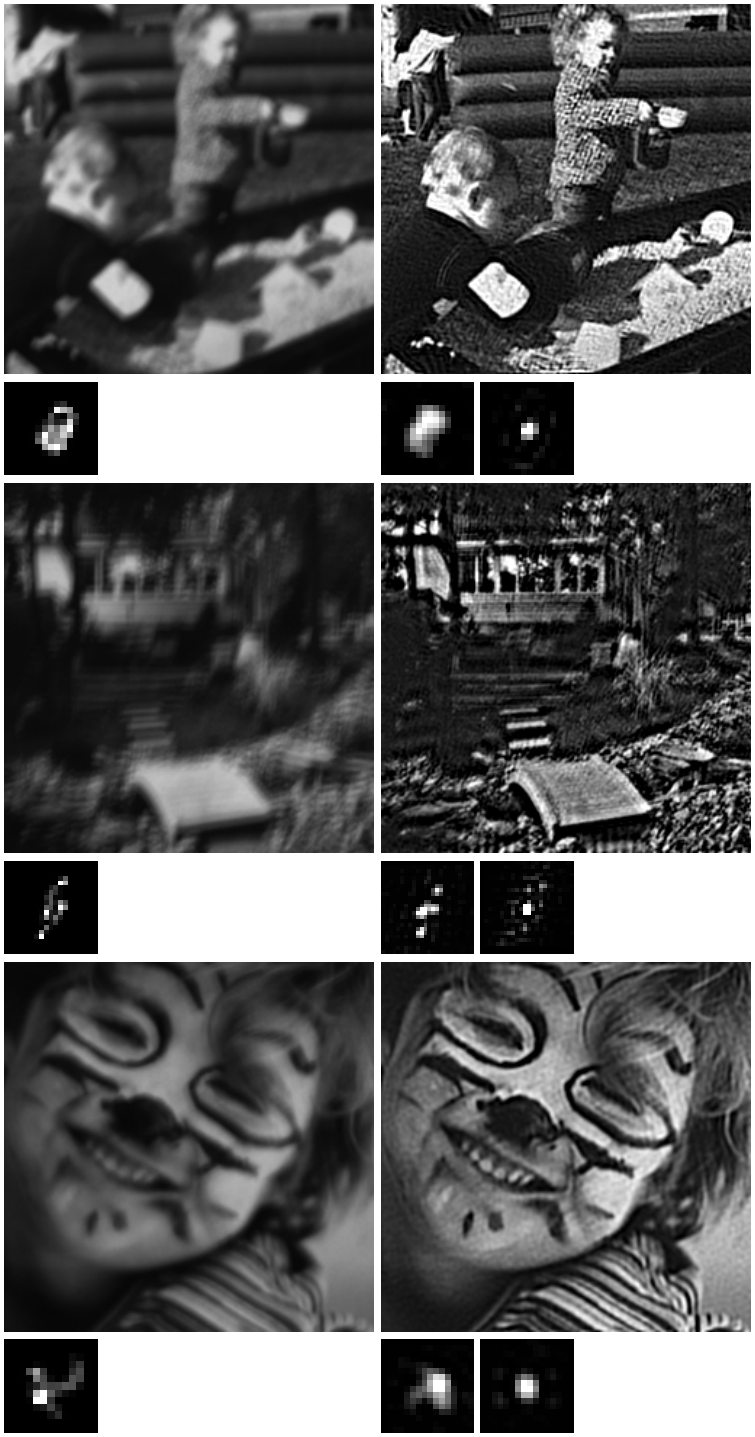

Fig. 6: Left column: blurred images. The true blur kernel is shown below each image. Right column: Our blind deconvolution result. The blur kernel estimated in the first iteration and the residual blur estimated in the second iteration are shown below each image. Dataset courtesy of [17].

plish. Successful results on a variety of challenging test cases demonstrate the robustness and visual quality of the suggested approach.

References

1. Kotera, J., Šroubek, F., Milanfar, P.: Blind deconvolution using alternating maximum a posteriori estimation with heavy-tailed priors. CAIP, LNCS 8048, 59–66 (2013)
2. Fergus, R., Singh, B., Hertzmann, A., Roweis, S.T., Freeman, W.T.: Removing camera shake from a single photograph. SIGGRAPH. 25, 787–794 (2006)
3. Ambrosio, L., Tortorelli, V.M.: Approximation of functionals depending on jumps by elliptic functionals via Γ-convergence. Communications on Pure and Applied Mathematics. 43, 999–1036 (1990)
4. Bar, L., Sochen, N., Kiryati, N.: Variational pairing of image segmentation and blind restoration. ECCV, LNCS 3022, 166–177 (2004)
5. Zheng, H., Hellwich, O.: Extended Mumford-Shah regularization in bayesian estimation for blind image deconvolution and segmentation. IWCIA, LNCS 4040, 144—158 (2006)
6. Shan, Q., Jia, J., Agarwala, A.: High-quality motion deblurring from a single image. SIGGRAPH. (2008)
7. Bar, L., Sochen, N., Kiryati, N.: Semi-blind image restoration via Mumford-Shah regularization. IEEE Transactions on Image Processing. 15, 483–493 (2006)
8. Zhu, X., Milanfar, P.: Stabilizing and deblurring atmospheric turbulence. ICCP. (2011)
9. Gal, R., Kiryati, N., Sochen, N.: Progress in the restoration of image sequences degraded by atmospheric turbulence. Pattern Recognition Letters. 48, 8–14 (2014)
10. Vogel, C.R., Oman, M.E.: Fast, robust total variation-based reconstruction of noisy, blurred images. IEEE Trans. Image Process. 7, 813-–824 (1998)
11. Zhou, Y., Komodakis, N.: A MAP-estimation framework for blind deblurring using high-level edge priors. ECCV, LNCS 8690, 142 – 157 (2014)
12. Mahpod, S., Yitzhaky, Y.: Compression of turbulence-affected video signals SPIE. 7444 (2009)
13. Oreifej, O., Li, X., Shah, M.: Simultaneous video stabilization and moving object detection in turbulence. IEEE Trans. PAMI. 35, 450 – 462 (2013)
14. Mumford, D., Shah, S.: Optimal approximations by piecewise smooth functions and associated variational problems. Commun. Pure and Appl. Math. 42, 577 – 682 (1989)
15. Wiener, N.: Extrapolation, interpolation, and smoothing of stationary time series. MIT Press. (1964)
16. Michaeli, T., Irani, M.: Blind deblurring using internal patch recurrence. ECCV, LNCS 8691, 783-798 (2014)
17. Levin, A., Weiss, Y., Durand, F., Freeman, W.T.: Understanding and evaluating blind deconvolution algorithms. CVPR (2009)
18. Gildenblat, J.: Fast GPU implementation of Mumford-Shah regularization Semi-blind image restoration. Unpublished M.Sc. project report. School of Electrical Engineering, Tel Aviv University (2012)
19. You, Y., Kaveh, M.: A Regularization Approach to Joint Blur Identification and Image Restoration. IEEE Trans. Image Processing, 5, 416–428 (1996)
20. Chan, T., Wong, C.: Total Variation Blind Deconvolution. IEEE Trans. Image Processing, 7, 370–375 (1998)